J | P | S | T

http://jpst.irost.ir

Journal of Particle Science and Technology

IROST

The effects of suspending medium on dielectrophoretic systems for separating and sorting carbon nanotubes

Razieh Beigmoradi[1,2,*], Seyed Foad Aghamiri[3]

[1] *Department of Chemical Engineering, Faculty of Engineering, University of Sistan & Baluchestan, Zahedan, Iran*

[2] *Innovation Center for Membrane Technology (ICMT), University of Sistan & Baluchestan, Zahedan, Iran*

[3] *Department of Chemical Engineering, Faculty of Engineering, University of Isfahan, Isfahan, Iran*

HIGHLIGHTS

- The separation of CNTs was studied in a DEP system based on electrical properties.
- The effect of seven solvents as suspending medium on the DEP system was investigated.
- The suspending medium has a direct influence on the design and optimization of DEP systems.
- Geometrical separation of CNTs based on their diameter is possible in the DEP system.

GRAPHICAL ABSTRACT

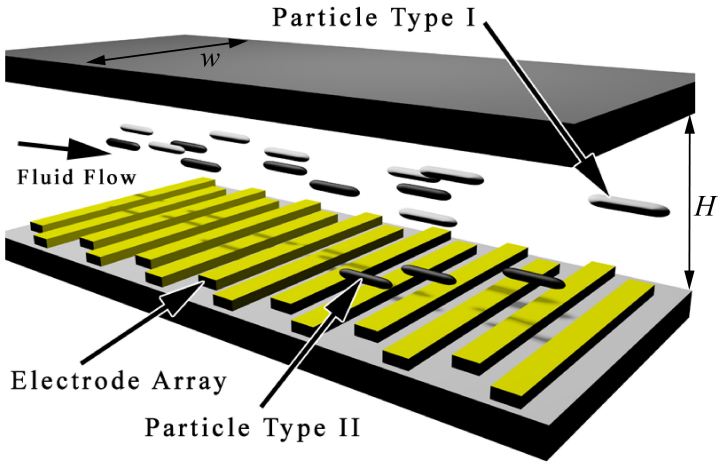

ARTICLE INFO

Article history:

Received 7 October 2019
Revised 6 December 2019
Accepted 10 December 2019

Keywords:

Carbon nanotubes
Dielectrophoresis
Separation and sorting
Suspending medium

ABSTRACT

The separation of two different types of multi-walled carbon nanotubes is studied in a dielectrophoresis-based microchannel system in seven different solvents as the suspending medium. A simple model was developed to predict the behavior of the multi-walled carbon nanotubes in the above mentioned system. Then, the equations of motion for the multi-walled carbon nanotubes in that system were introduced and the effect of the suspending medium type on the fabrication parameters of dielectrophoretic system, such as applied voltage and inter electrode gap, was surveyed. The calculations indicate that the suspending medium has a direct influence on the design and optimization of dielectrophoretic systems. The geometrical separation of the carbon nanotubes is considered here, and it was found that the model predicts some advantages in separation and sorting multi-walled carbon nanotubes based on their diameter.

* *Corresponding author: Tel.: +98913-3794960 ; Fax: +9854-33447092 ; E-mail address: beigmoradi@pgs.usb.ac.ir*

DOI: 10.22104/JPST.2019.3848.1157

1. Introduction

Due to their interesting electrical properties, carbon nanotubes (CNTs) are recognized as outstanding materials for electrical applications, i.e., sub-micrometer electronic devices [1,2]. Since both metallic and semiconducting CNTs are produced simultaneously they need to be separated for specific applications. Many diverse methods have been proposed for this purpose [3-8].

Dielectrophoresis (DEP) is one of the most successful methods to separate and manipulate CNTs. DEP is the phenomenon, first introduced by Pohl [9], where a force is implied on a dielectric particle when it is subjected to a non-uniform electric field. All particles exhibit dielectrophoretic activity in the presence of non-uniform electric fields. The particles with more polarizability than that of the suspending medium move toward the stronger area of the field, which is called positive DEP; negative DEP is where the particles with low polarizability move away from the strong field region [10]. This phenomenon causes the suspended particles to move in opposite directions, known as the directional separation. Krupke *et al.* were the first who used this phenomenon to deposit metallic CNTs onto microelectrodes [11]. They applied an electric field of about 2×103 V/cm and revealed that the dielectrophoretic system was able to separate or categorize the CNTs into metallic and semiconducting categories. Parameters which effect DEP systems, such as frequency, applied voltage, and electrode geometry, has been studied to separate and manipulate CNTs [12-16].

Since the strength and direction of the DEP force depends on the difference between the complex permittivity available between the particle and the suspending liquid medium, the effect of the medium should be considered as one of the most important parameters in a DEP system. A good understanding of the suspending medium effect is the key to using DEP systems to control the sorting process [17-19]; although, research focusing on the role of this parameter to sort and assembly CNTs is still limited.

The main objective of this study is the investigation of the effect of seven different solvents used as mediums on the behavior of two types of CNTs with different electrical properties in a DEP system. The equations of motion of the multi-walled carbon nanotubes (MWCNTs) were then obtained in a DEP system. These equations were applied to study the directional separation phenomenon, sorting and trajectory of MWCNTs in a DEP system when different solvents were used as the medium.

2. Theory

When particles are placed in an electric field (E), a grate dipole moment is induced in the particles and a force (F) is applied on the dipole. A well-known expression for this force, where P is the polarization vector, is presented as Eq. (1) [20].

$$F = (P.\nabla)\, E \tag{1}$$

where, the higher-order terms of the force are omitted [21].

According to equation (1) the time average DEP force on the dipole of the particle is derived as Eq. (2) [22]

$$F_{DEP} = 1/4\ \upsilon \mathrm{Re}[\tilde{\alpha}_n]\nabla|E|^2 \tag{2}$$

where υ and $\nabla|E|^2$ are the volume of the particle and the gradient of the electric field amplitude squared, respectively. CNTs shape can be considered as a prolate ellipsoid ($a>>b = c$, where a, b and c are half lengths along the coordinate axes). A geometrical factor (Γ), based on the volume of an ellipsoid (υ = 4/3 abc), can be defined for the CNT with the radius r and length ℓ such as Eq. (3):

$$\Gamma = \frac{1}{4}\upsilon_{\text{Prolate ellopsoid}} = \frac{\pi}{6} r^2 \ell \tag{3}$$

$\tilde{\alpha}_n$ is the complex polarizability given by $\tilde{\alpha}_n = \varepsilon_m \tilde{K}_n$ for an ellipsoid. Here, ε_m and $\tilde{K}_n$ are the real part of the complex permittivity of the suspending medium and the Clausius-Mossotti factor equivalent along axis n (where n = 1, 2, 3), respectively [21]. The $\tilde{K}_n$ depends on the frequency presented by:

$$\tilde{K}_n = \frac{\tilde{\varepsilon}_p - \tilde{\varepsilon}_m}{A_n\left(\tilde{\varepsilon}_p - \tilde{\varepsilon}_m\right) + \tilde{\varepsilon}_m}$$

where $\tilde{\varepsilon}_m$ and $\tilde{\varepsilon}_p$ refer to the complex dielectric permittivity of the medium and particle, respectively, defined as:

$$\tilde{\varepsilon}_j = \varepsilon_j - i\left(\frac{\sigma_j}{\omega}\right) \quad (j = m, p)$$

in which σ and ω are the conductivity and angular

frequency, respectively. An is called the depolarizing factor along the *n* axis tending to zero when the major axis of the prolate ellipsoid is aligned with the field [21]. In this case, the major axis of the CNT is its length; therefore, the complex polarizability is presented as Eq. (4):

$$\tilde{\alpha} = \varepsilon_m \frac{\tilde{\varepsilon}_p - \tilde{\varepsilon}_m}{\tilde{\varepsilon}_m} \tag{4}$$

Combining Eqs. (3) and (4) with Eq. (2) gives the dielectrophoretic force on a CNT when the major axis and the electric field have the same direction (Eq. (5)).

$$F_{DEP} = \Gamma\, \varepsilon_m\, \mathrm{Re}\left\{\frac{\tilde{\varepsilon}_p - \tilde{\varepsilon}_m}{\tilde{\varepsilon}_m}\right\} \nabla |E|^2 \tag{5}$$

It is known that all other orientations are unstable positions [22,23], so that the simple assumption the major axis will always be aligned with the line field can be made. Therefore, Eq. (5) will be valid for the dielectrophoretic behavior of the CNT which experiences positive force.

In Eq. (5), the term $f_{\mathrm{C.M}} \equiv \frac{(\tilde{\varepsilon}_p - \tilde{\varepsilon}_m)}{\tilde{\varepsilon}_m}$ is known as the equivalent of the Clausius-Mossotti factor for a spherical shape. The real part of $f_{\mathrm{C.M}}$ can be simplified in the following expressions for low and high frequency limits, respectively [21].

$$\mathrm{Re}\{f_{\mathrm{C.M}}\} = \frac{\sigma_p - \sigma_m}{\sigma_m} \quad \text{as} \quad \omega \to 0 \tag{6a}$$

$$\mathrm{Re}\{f_{\mathrm{C.M}}\} = \frac{\varepsilon_p - \varepsilon_m}{\varepsilon_m} \quad \text{as} \quad \omega \to \infty \tag{6b}$$

Since the electrical properties (both the particles and the medium) in $\mathrm{Re}\{f_{\mathrm{C.M}}\}$ depend on the frequency, a useful relationship can be obtained by using the cross-over frequency technique [24] as follows:

$$f_{\mathrm{C.O}} = \frac{1}{2\pi} \sqrt{-\frac{(\sigma_p - \sigma_m)\sigma_m}{(\varepsilon_p - \varepsilon_m)\varepsilon_m}} \tag{7}$$

where, $f_{\mathrm{C.O}}$ is a frequency in which particles are stationary in spite of the exerting field, known as the cross-over frequency. This frequency distinguishes the negative and positive DEP force regions.

3. Modeling of the DEP system

To investigate the separation and sorting of CNTs in different media with the DEP technique, a microchannel was considered with *w* width, *H* height, and an interdigitated electrode array with an interelectrode gap with width d in the bottom of the channel (see Fig. 1).

The most important forces a particle is exposed to in the DEP system are buoyancy and drag forces, while the near-wall forces and particle-particle interactions are ignored. According to Newton's second law, the equation of motion for a particle in the vertical direction is:

$$\sum F_y = m_p \frac{du_y}{dt} = F_{DEP,y} + F_{Buoyancy} + F_D \tag{8}$$

where F_{DEP}, F_B and F_D are dielectrophoresis force, buoyancy force, and drag force, respectively. The stochastic forces can be disregarded provided $F_{DEP} \geq 3/2\, k_B T$ (k_B is the Boltzmann's constant) [25]. The buoyancy and drag forces are defined by the following equations, respectively:

$$F_{buoyancy} = (\rho_p - \rho_m)\, v_p g \tag{9}$$

$$F_D = -f u \tag{10}$$

where *f* is the time average friction factor of the CNT, regarded as a prolate ellipsoid moving in a chaotic manner in a liquid with the viscosity of η [21],

$$f = \frac{3\pi\eta\ell}{\ln(\ell/r)} \tag{11}$$

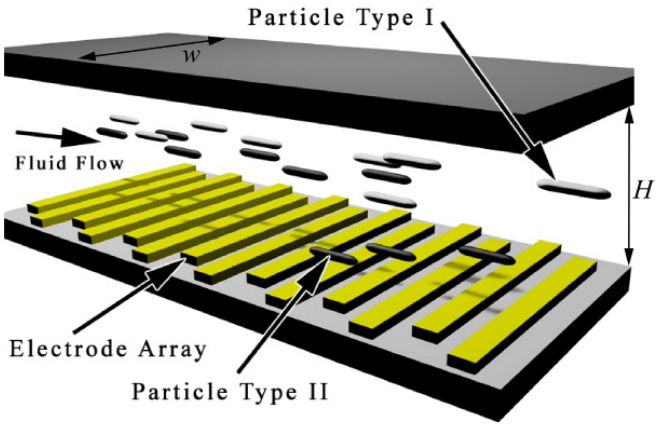

Fig. 1. The schematic diagram shows the principle of operation of a simple dielectrophoretic separator. As the mixture flows across the electrode array, type II MWCNT experience positive DEP and are attracted to the electrodes. They separate from type I MWCNT which experience negative DEP (or no force) and are repelled from the electrodes and pass through the channel.

By substituting Eqs. (9) and (10) into Eq. (8), the Eq. (12) will be obtained.

$$\frac{du_y}{dt}=\frac{F_{DEP}}{m_p}+\left(\frac{\rho_p-\rho_m}{\rho_p}\right)g-\frac{f}{m_p}u_y \tag{12}$$

This equation can be solved analytically by applying an appropriate initial condition. If the initial velocity is chosen to be equal to zero, Eq. (12) can be solved for u_y as follows:

$$u_y=\left(\frac{F_{DEP}}{f}+\frac{\gamma_B g}{\zeta}\right)\left(1-exp\left(-\zeta t\right)\right) \tag{13}$$

where $\zeta\equiv\frac{f}{m_p}$, and $\gamma_B=\frac{\left(\rho_p-\rho_m\right)}{\rho_p}$ is the buoyancy force constant.

To calculate the DEP force, the gradient of the electric field amplitude squared term should be determined analytically or numerically. In this article, the following analytical expression is used for the mentioned electrode arrays geometry[26]:

$$\nabla\left|E\right|^2=\frac{V_0^{\,2}}{d^3}\frac{32}{\pi}exp\left(-\frac{\pi y}{d}\right) \tag{14}$$

where V_0 is the applied potential and y is the particle distance above the surface of the electrode array.

The horizontal velocity of the particles (u_x) in the channel is presented by the following equation for a fully developed parabolic flow profile [27]:

$$u_x=-\frac{6Q}{Hw}\left(\left(\frac{y}{H}\right)^2-\left(\frac{y}{H}\right)\right) \tag{15}$$

where, Q is the volume flow rate of the fluid. Eq. (15) is obtained when the horizontal velocity at the top and bottom of the channel is zero.

Eqs. (13) and (15) present the particle trajectory of CNTs. Two main assumptions were used for the derivation of Eq. (15): the horizontal component of DEP and the electro-osmosis velocity ($u_{electroosmosis}$) are negligible. The electro-osmosis velocity is the local fluid motion generated near the electrode edges because the AC field acts on the medium as well as the particles. The time average electro-osmosis velocity of the fluid based on a circuit model has been derived for a simple electrode geometry consisting of thin parallel plates fabricated on an isolating substrate and a narrow gap as Eq. (16) [21].

$$u_{electroosmosis}=\frac{1}{8}\frac{\varepsilon_m V_0^2\Omega^2}{\eta x\left(1+\Omega^2\right)^2} \tag{16}$$

where x is the distance from the electrode edge, $\Omega=(1/2)\pi\kappa x\left(\frac{\varepsilon}{\sigma}\right)\omega$ is the non-dimensional frequency, and κ is the reciprocal Debye length. According to Eq. (16), this velocity tends towards zero at high frequencies. In this study, Eq. (16) can be used to estimate the electro-osmosis velocity because of the similarity in the mentioned electrodes geometry and interdigitated electrodes shapes.

4. Results and discussion

4.1. The directional separation of MWCNTs

To study the dielectrophoretic separation and sorting of CNTs, we considered two samples of MWCNTs with the electrical properties presented in Table 1 [24]. The suspended MWCNTs were injected into a DEP channel with a 10 μm-height and 100 μm-width.

An electrode array with 1.5 μm width and 1.5 μm spacing (gap) was inserted in the bottom of the channel. Calculations were made for seven solvents to study the effect of the suspending medium. The most important properties of the solvents are presented in Table 2. It was experimentally found that these selected seven suspending media cause a stable suspension of the CNTs.

The real part of the equivalent Clausius-Mossotti factor ($\mathrm{Re}\{f_{\mathrm{C.M}}\}$) vs. frequency ($f$) are shown in Figs. 2(a)-2(g), when two MWCNTs with the different effective polarizabilities are dispersed in the solvents. These figures demonstrate a different DEP behavior for the two particles. These figures indicate that for all solvents, there is a range of frequencies where one type of MWCNTs experiences positive DEP while the other experiences negative DEP. According to Figs. 2(a)-2(d), type II MWCNT exhibit a positive $\mathrm{Re}\{f_{\mathrm{C.M}}\}$ in IPA, DMF, ethanol and acetone in all frequencies (from 100 to 0.1GHz). This means that the particle always

Table 1. Electrical properties of the studied samples [24].

Particles	**MWCNT**	
	Type I	**Type II**
Permittivity (F/m)	$18.44\varepsilon_0$	$2.2\times10^{+3}\varepsilon_0$
Conductivity (S/m)	1.58×10^{-2}	3.12×10^{-3}

Table 2. The physical properties of the solvents used as suspending media to seperate the MWCNTs.[a, b]

Media	Molecular Weight (gr/mole)	Density (gr/cm^3)	Viscosity (mPa.s)	Electrical Conductivity (S/m)	Permittivity (F/m)	Diffusion Coefficient (cm^2/s)
Isopropyl Alcohol (IPA)	60.1	0.786	2.5	6.0×10^{-6}	18.6	5.46×10^{-6}
Sodium Dodecyl Sulfonate (SDS)	288.4	1.01	1	0.125	80	4.52×10^{-6}
Dodecyl Benzene Sulfonate Acid (BSA)	354.1	1.06	1.7	0.004	3900	2.505×10^{-6}
Dichloroethylene (DCE)	96.9	1.26	0.404	0.0124	2.15	3.348×10^{-5}
N,N-Dimethyl formamide (DMF)	73.1	0.945	0.8	6.00×10^{-6}	36	2.70×10^{-5}
Acetone	58.1	0.791	0.33	5.50×10^{-6}	21.58	3.50×10^{-5}
Ethanol	46.1	0.789	1.19	1.40×10^{-7}	22.4	1.67×10^{-5}

[a] The properties of the solvents from [28-32].

[b] The diffusion coefficients from [33-37].

experiences a positive DEP force; consequently, it moves towards the electrode edge. But type I MWCNT experience negative DEP force at higher frequencies than the cross-over frequency. Therefore, these two types of MWCNTs can be separated directionally.

Figs. 2(e) and 2(f) indicate that the directional separation of types I and II MWCNT happened at low frequencies. In DCE (Fig. 2(e)), the $\mathrm{Re}\{f_{\mathrm{C.M}}\}$ is positive after 2.81 MHz for type II. Therefore, both particles types experience the DEP force with the same sign and move towards the electrode edge at high frequencies. The behavior of the two types of particles in DBSA (Fig. 2(f)) is similar to DCE at low frequencies, but a difference occurs at the high range where both particles escape by moving away from the electrode regions.

The results for SDS are shown in the final figure. Here the directional separation occurs at high frequencies, similar to Figs. 2(a)-2(d). It should be noted that in the SDS solvent both types of dispersed MWCNTs experience the negative DEP force in contrast to the IPA, acetone, ethanol and DMF solvents at low range frequencies. According to Eq. (5), the magnitude of the DEP force is proportional to $\mathrm{Re}\{f_{\mathrm{C.M}}\}$. A sharp separation can occur when the difference among $\mathrm{Re}\{f_{\mathrm{C.M}}\}$ of the particles is great. This point is explained more clearly in Table 3. According to Table 3, the directional separation of the MWCNTs is sharper in the IPA solvent than the other solvents. This point is an important feature in the design of a DEP system. This theoretical analysis is confirmed by other experimental observations [14,18].

Table 3. The difference between the real part of the Clausius-Mossotti factor for type I and type II MWCNT, where the sign of $\mathrm{Re}\{f_{\mathrm{C.M}}\}$ for both types is opposite and free from frequency.

Media	$\lvert\mathrm{Re}\{f_{C.M}\}_{\text{type II}}\rvert - \lvert\mathrm{Re}\{f_{C.M}\}_{\text{type I}}\rvert$
IPA	117.288
Acetone	101.092
Ethanol	97.391
DMF	60.599
SDS	27.269

The important points of these diagrams are summarized in Table 4, which presents the sign of $\mathrm{Re}\{f_{\mathrm{C.M}}\}$ at low and high range frequencies. Moreover, the value of the cross-over frequency ($f_{\mathrm{C.O}}$) is calculated by Eq. (7). The absence of $f_{\mathrm{C.O}}$, is indicated by NA. These data indicate that electrical properties of the medium (conductivity or permittivity) play a primary role in the magnitude of the cross-over frequency.

These two MWCNTs behave in the media differently. For example type I may be attracted to an electrode in DCE while it escapes from the region in other solvents at high frequencies [37]. This may alter the judgment of the electrical properties of the CNTs based on the attraction or repulsion of the CNT in the DEP system.

On the other hand, this behavior is an important difference between these real MWCNTs and the metallic SWCNTs (m-SWCNTs). It is known that m-SWCNTs often have positive $\mathrm{Re}\{f_{\mathrm{C.M}}\}$ and they experience the positive DEP force. Likewise, m-SWCNTs can be attracted to the electrode edges while the semiconducting

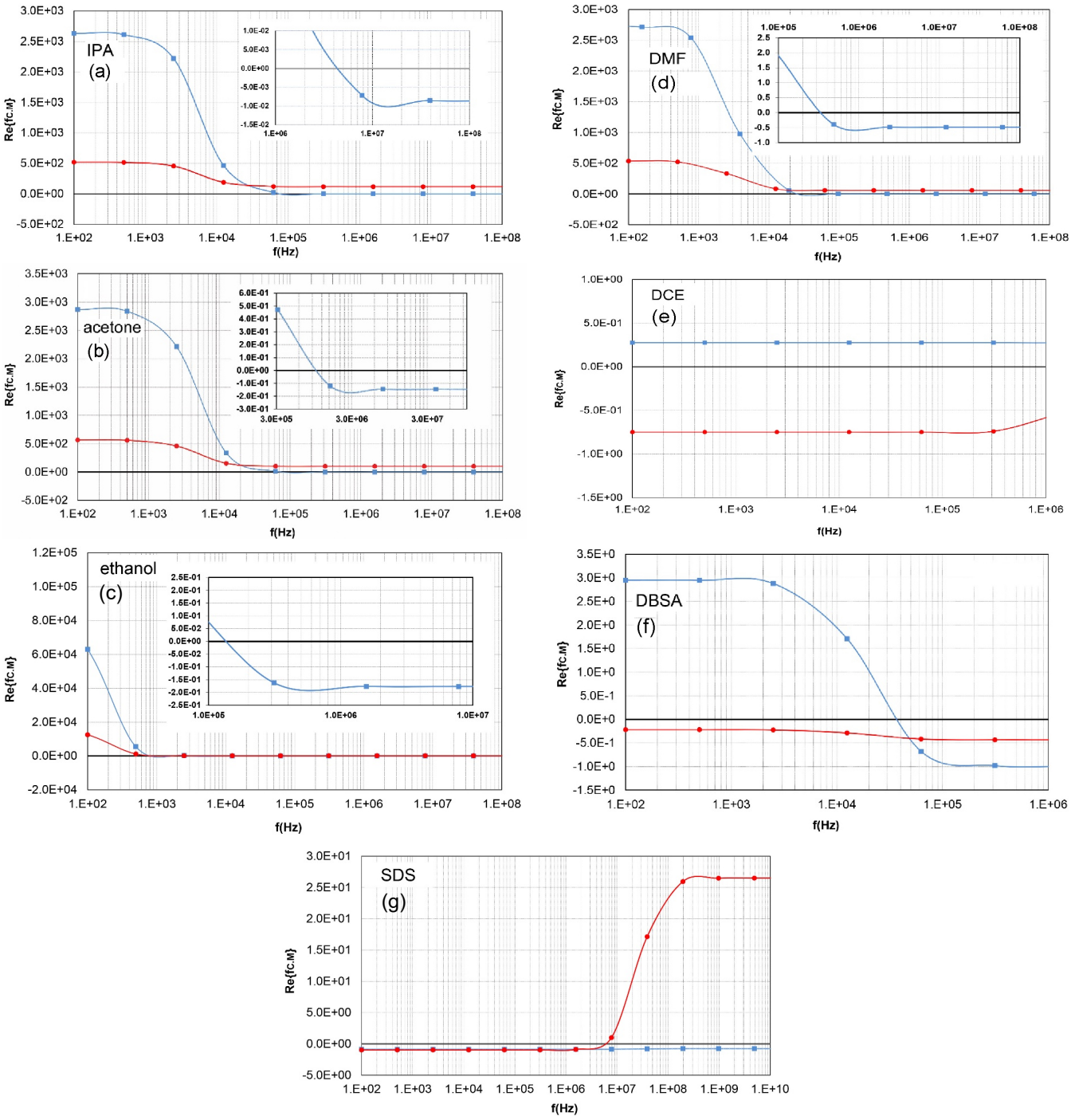

Fig. 2. Plot of Re$\{f_{C.M}\}$ for two MWCNTs vs. frequency in (a) IPA, (b) acetone, (c) ethanol, (d) DMF, (e) DCE, (f) DBSA and (g) SDS solvent: Type I (■) and Type II (●). The schematic diagram shows the principle of operation of a simple dielectrophoretic separator. As the

single walled carbon nanotubes (s-SWCNTs) are repulsed. This may indicate that MWCNTs do not have an absolute metal property.

Fig. 3 shows the electroosmosis velocity calculated by Eq. (16). It determines the electroosmosis velocity is important only at low frequencies (<1 MHz) where the effective frequency range for the DEP separation is significantly higher than 1 MHz. This figure confirms that this phenomenon can be negligible in the range of frequency considered in this study.

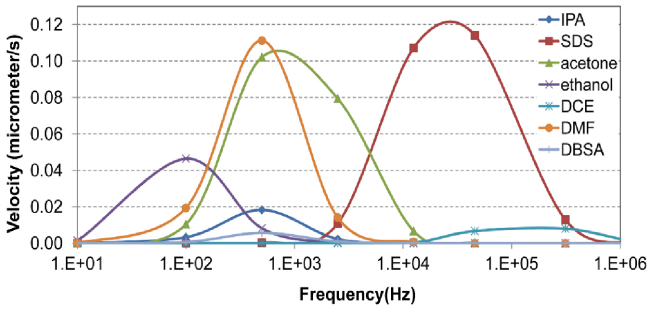

Fig. 3. Electroosmosis velocities of the all of solvents as a function of frequency.

Table 4. The sign of Re$\{f_{C.M}\}$ at low (f_l) and high (f_h) range frequencies and the cross-over frequency ($f_{C.O}$) for two types of the MWCNTs in different suspending media.

Media	Type I[a]			Type II[a]		
	Sign of Re$\{f_{C.M}\}$ at f_l	$f_{C.O}$	Sign of Re$\{f_{C.M}\}$ at f_h	Sign of Re$\{f_{C.M}\}$ at f_l	$f_{C.O}$	Sign of Re$\{f_{C.M}\}$ at f_h
IPA	+	3.21×10^6	-	+	NA	+
Acetone	+	6.44×10^5	-	+	NA	+
Ethanol	+	8.98×10^4	-	+	NA	+
DMF	+	2.18×10^5	-	+	NA	+
DCE	+	NA	+	-	2.81×10^6	+
DBSA	+	3.18×10^4	-	-	NA	-
SDS	-	NA	-	-	5.39×10^6	+

[a] Referred to Table 1.

4.2. The trajectory of the MWCNTs

The particle trajectory in SDS solvent is simulated by the simultaneous numerical solution of Eqs. (13) and (15). According to the boundary conditions, the particle is put above the channel while the vertical and horizontal components of the velocity are zero. The results for a MWCNT with a 20 nm diameter and 0.5 μm length passing through a 10×100 μm^2 channel cross section are presented in Fig. 4. The channel has parallel bar electrodes with 1.5 μm width and 1.5 μm gap on the base, and its applied voltage is 10 V. The flow rate is selected as 75 $\mu m^3/s$. Fig. 4 indicates that the MWCNT moved down to the edge of the electrode attracted by the DEP force, similar to other experimental evidence [38,39].

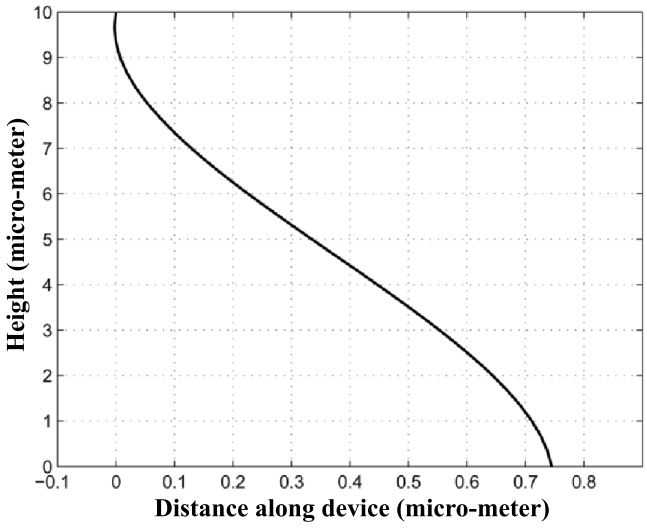

Fig. 4. Moving path of a MWCNT in a 10 μm-high (H) and 100 μm-wide (w) DEP channel above one interdigitate electrode, attracted under a positive DEP force.

4.3. The effect of the suspending medium on particles' movement

The vertical velocity of the type II MWCNT is calculated to study the effect of the suspending media. According to Table 4, this type experienced positive DEP force in all suspending media at high frequencies.

The velocity of the type II MWCNT for five different media is shown in Fig. 5 as a function of vertical position towards the surface of the electrode. As indicated in the figure, the particle velocity increases exponentially as (y/H) is reduced and the particle approaches the electrode surface. This behavior is expected since the DEP force decreases exponentially as the distance from the electrode surface increases (see Eqs. (5) and (14)).

The gradient of the electric field amplitude squared ($\nabla|E|^2$) is shown in Fig. 6 for the five solvents for the

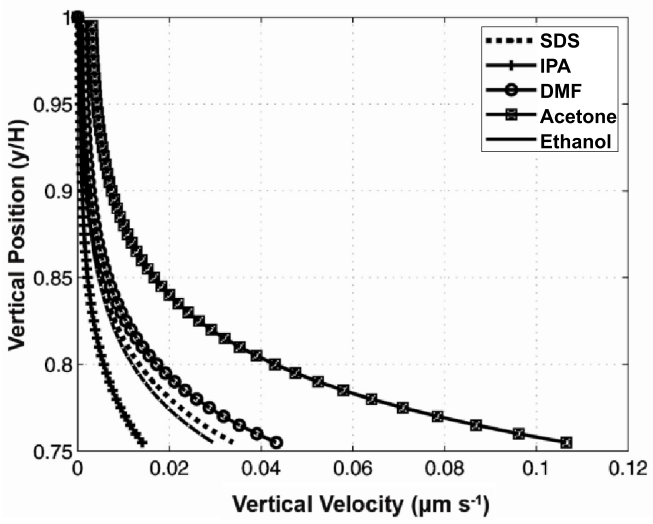

Fig. 5. The velocity of the type II MWCNT as a function of vertical position toward the surface of the electrode in the suspending media.

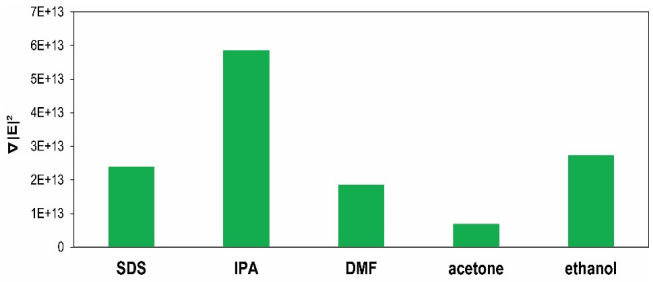

Fig. 6. The gradient of the electric field amplitude squared the MWCNT with a diameter of 20 nm and length of 0.5 μm passing through a 10×100 μm^2 channel cross section with a particle velocity of 0.02 μm/s.

same particle velocity. The results were calculated with a particle velocity of 0.02 μm/s. According to Figs. 5 and 6, it can be deduced that the exerted force on a MWCNT in the DEP-based microchannel system and the resulting particle movement can be controlled by the characteristics of the given medium [18].

4.4. The effect of fabrication parameters on DEP proceeds with respect to suspending media

Since $\nabla|E|^2$ is a function of applied voltage and interelectrode gap (Eq. (14)), these parameters can be adjusted to satisfy convenient conditions for separation. In this section the voltage and electrode gap were determined for five solvents, where a MWCNT moves with the same velocity in the all of solvents. The applied voltage and electrode gap are shown in Figs. 7 and 8, respectively.

These figures confirm that the appropriate choice of solvent can improve a DEP system performance. For instance, to move the MWCNT at 0.02 μm/s the applied voltage in acetone is 6.7 V while it is 19.5 V in IPA (Fig. 6). This means that the required energy in a DEP system using acetone is lower than that in a DEP system using IPA. In another case (Fig. 7), when acetone is the

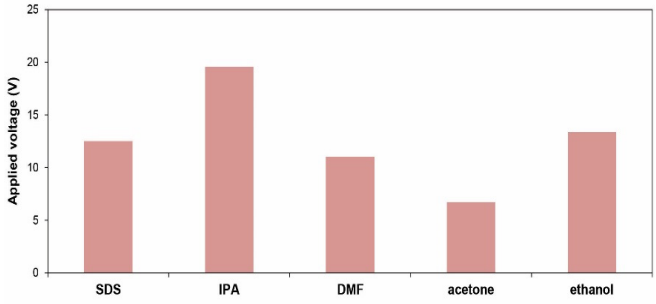

Fig. 7. The comparison of applied voltage in the DEP system for different suspending media.

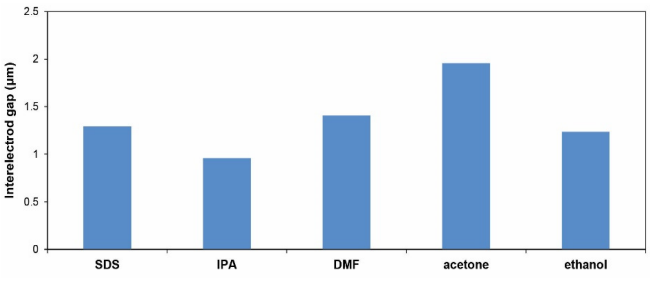

Fig. 8. The comparison of inter electrode gap in the DEP system for different suspending media.

surrounding medium, the inter electrode gap is about 2 μm to move the MWCNT at 0.02 μm/s while it would be ~1.2 μm for ethanol. So in the large scale, a DEP system with 100 electrodes using ethanol is ~80 μm smaller than the same DEP system using acetone. These findings could have great benefits in future of the lab-on-a-chip (LOP) technologies.

4.5. Sorting the MWCNTs by DEP system

The vertical velocity of MWCNTs depends on particle size (see Eqs .(2), (11), and (13)). It reveals that particles with different dimensions can be separated in a DEP system in spite of similar dielectric properties.

The vertical velocities (u_y) indicated in Figs. 9(a)-9(d). u_y are calculated for three MWCNTs with diameters of 20, 60 and 100 nm vs. vertical position (y/H) for three voltages and two electrode gaps. It is observed that the three MWCNTs are moving with different speeds through the same fluid medium. Therefore, their sorting is possible.

However, the developed DEP devices does not provide the continuous separation of particles based on the size. They can be achieved by using a multistep strategy [40,41].

5. Conclusion

In this article, the separation of CNTs is studied in a DEP system based on electrical properties. This work focuses on the benefits of choosing the appropriate suspending medium in the DEP systems for electrical- and size-based separation of CNTs.

The results indicate that the properties of the solvent are the important key factors in the CNTs separation based on electrical properties. This means that a CNT can be attracted by electrodes in a specific solvent, while it can be repelled in another solvent. In fact, attraction

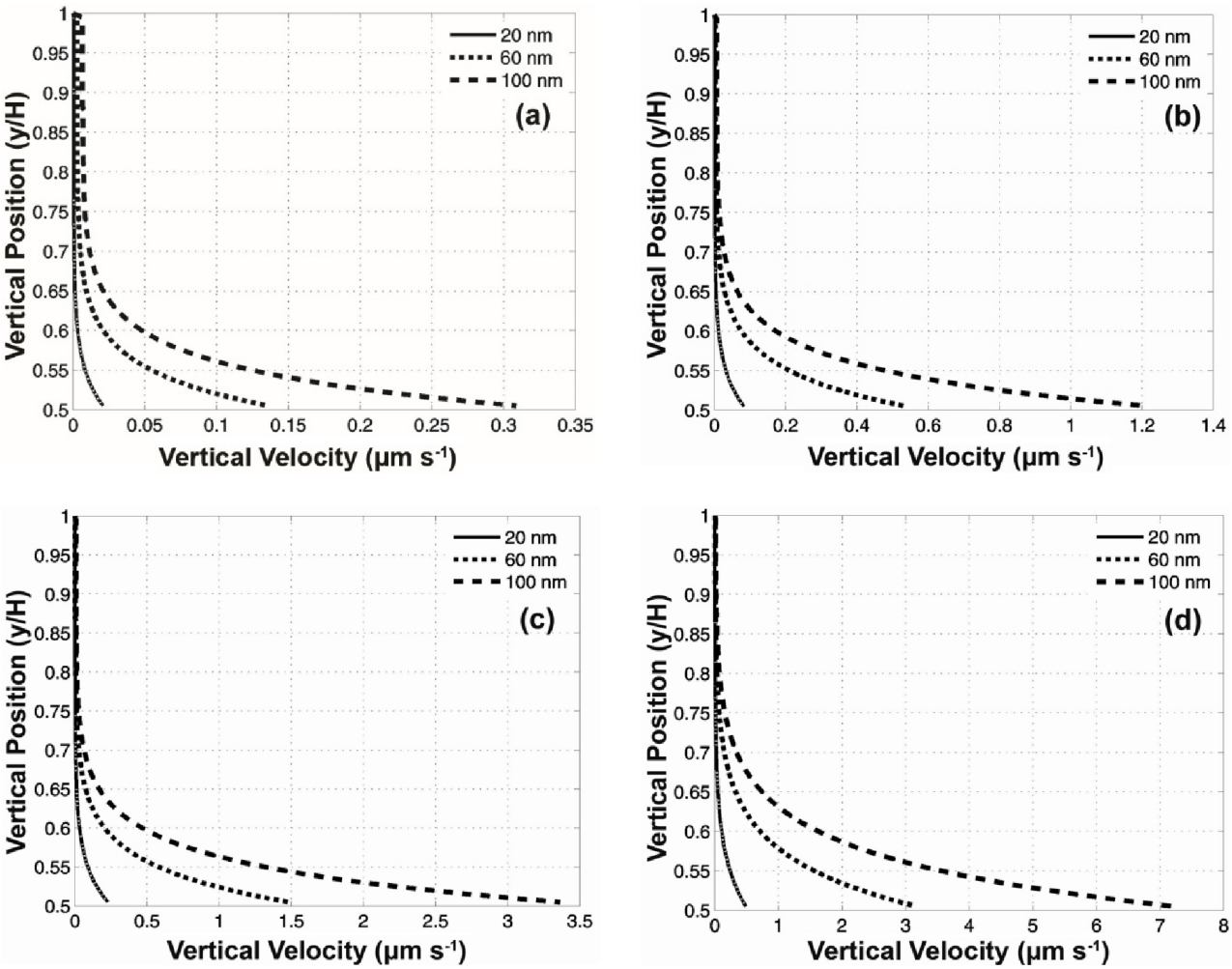

Fig. 9. The vertical velocities of the MWCNTs with different sizes (20, 60 and 100 nm in diameter) in the DEP system with an inter electrode gap of 1.5 μm and an applied voltages of 3 (a), 6 (b), and 10 V (c). Also, the vertical velocities have been calculated in the applied voltage of 6 V and the inter electrode gap of 2 μm (d), which is comparable with the result in (b).

or repulsion of the CNTs, which is referred to as their metallic or the semiconducting properties, depends on the suspending medium properties. One simple model is proposed to predict the behavior of a CNT in a micro channel where the particle is exposed to a positive DEP force, and the related equations were derived. The effect of various parameters, such as the diameter of the CNT, solvent properties, applied voltage and inter electrode gap, are investigated on directional separation and sorting of CNTs. The model results emphasize that the suspending medium is a vital factor in the DEP system. The appropriate selection of the surrounding medium can contribute to better. DEP system design and enhance the efficiency. Accordingly, designing a multistep DEP system for size-based separation of the CNTs becomes possible.

Nomenclature

Symbol	Notes	Units	Base units
A_n	Depolarizing factor along axis n		-
a, b, c	Particle radius		m
d	Distance		m
E	Electric field	$V.m^{-1}$	$A^{-1}.kg.m\ s^{-3}$
F	Force	N	$Kg.m.s^{-2}$
$F_{Buoyancy}$	Buoyancy force	N	$Kg.m.s^{-2}$

Symbol	Notes	Units	Base units
F_D	Drag force	N	$Kg.m.s^{-2}$
F_{DEP}	Dielectrophoretic force	N	$Kg.m.s^{-2}$
f	Time average friction factor	-	$kg.s^{-1}$
$f_{C.M}$	Clausius-Mossoti factor	-	-
$f_{C.O}$	Cross-over frequency	Hz	s^{-1}
g	Gravitational acceleration	-	$m.s^{-2}$
H	Microchannel height	-	m
i	Complex unit ($i^2 = -1$)	-	-
$\tilde{K}_n$	Clausius-Mossoti factor equivalent along axis n	-	-
k_B	Boltzmann constant= 1.3806503E-23	-	$J.K^{-1}$
l	CNT length	-	-
m	(subscript) medium	-	-
m_p	Particle mass	-	kg
P	Polarization	$C.m^{-2}$	$A.m^{-2}.s$
p	(subscript) particle	-	-
Q	Volume flow rate	-	$m^3.s^{-1}$
r	CNT radius	-	m
T	Temperature	-	K
t	Time	-	s
u	Particle velocity	-	$m.s^{-1}$
V_0	Eclectic potential difference	V	$A^{-1}.kg.m^2.s^{-3}$
w	Microchannel width	-	m
x	x coordinate	-	-
y	y coordinate	-	-
y	(subscript) y component of vector	-	-
$\tilde{\alpha}$	Complex polarisability	$F.m^2$	$A^2.kg^{-1}.s^4$
$\tilde{\alpha}_n$	Complex polarisability along axis n	$F.m^2$	$A^2.kg^{-1}.s^4$
ε	Permittivity	$F.m^{-1}$	$A^2.kg^{-1}.m^{-3}.s^4$
$\tilde{\varepsilon}$	Complex permittivity	$F.m^{-1}$	$A^2.kg^{-1}.m^{-3}.s^4$
ε_0	Permittivity of free space constant =8.854187817E-12	$F.m^{-1}$	$A^2.kg^{-1}.m^{-3}.s^4$
γ_B	Buoyancy force constant	-	-
η	Viscosity	poise	$kg.m^{-1}.s^{-1}$
κ	Reciprocal debye length	-	m^{-1}
ρ_m	Mass density	-	$kg.m^{-3}$
ρ_p	Particle mass density	-	$kg.m^{-3}$
σ	Conductivity	$S.m^{-1}$	$A^2.kg^{-1}.m^{-3}.s^3$
υ	Volume	-	m^3
ω	Angular frequency	-	$rad.s^{-1}$
ξ	Reciprocal characteristic time constant	-	s^{-1}
Γ	Geometrical factor	-	m^3
Ω	Dimensionless frequency	-	-

References

[1] Y. Cao, S. Cong, X. Cao, F. Wu, Q. Liu, M.R. Amer, C. Zhou, Review of electronics based on single-walled carbon nanotubes, in Single-Walled Carbon Nanotubes: Springer, 2019, pp. 189-224.

[2] G. Rahman, Z. Najaf,A. Mehmood, S. Bilal, A.H. Ali Shah,S. Ahmad Mian, G. Ali, An overview of the recent progress in the synthesis and applications of carbon nanotubes, C-J. Carbon Res. 5, (2019) 3.

[3] S. Banerjee, T. Hemraj-Benny, S.S. Wong, Routes towards separating metallic and semiconducting nanotubes, J. Nanosci. Nanotechno. 5 (2005) 841-855.

[4] L. Kurzepa, A. Lekawa-Raus, J. Patmore, K. Koziol, Replacing copper wires with carbon nanotube wires in electrical transformers, Adv. Funct. Mater. 24 (2014) 619-624.

[5] C. Rinaldi, An invariant general solution for the magnetic fields within and surrounding a small spherical particle in an imposed arbitrary magnetic field and the resulting magnetic force and couple, Chem. Eng. Commun. 197 (2009) 92-111.

[6] H. Zhang, L. An, Progress in dielectrophoretic assembly of carbon nanotubes for sensing application, in MATEC Web of Conferences, 67 (2016) 06071.

[7] Q. Zhao, Z. Wang, L. Tong, Z. Zheng, W. Hu, J. Zhang, Selective sorting of metallic/semiconducting single-walled carbon nanotube arrays by 'igniter-assisted gas-phase etching', Mater. Chem. Front. 2, (2018) 157-162.

[8] M. Zheng, Sorting carbon nanotubes, in Single-Walled Carbon Nanotubes: Springer, 2019, pp. 129-164.

[9] H.A. Pohl, Dielectrophoresis: The behavior of neutral matter in nonuniform electric fields, Cambridge Monographs on Physics, Cambridge University Press, Cambridge, 1978.

[10] M.P. Hughes, Nanoelectromechanics in Engineering and Biology, CRC press, NY, 2002.

[11] R. Krupke, F. Hennrich, H.V. Löhneysen, M.M. Kappes, Separation of metallic from semiconducting single-walled carbon nanotubes, Science, 301 (2003) 344-347.

[12] S. Ammu, D.R. Heskett, The role of electric field and ultrasonication in the deposition and alignment of sngle-walled carbon nanotube networks using dielectrophoresis, World J. Cond. Mat. Phys. 3 (2013) 159-163.

[13] M.V. Gorshkov, A.S. Moskalenko, M.V. Shcherbak, Alternating electric field effect on the alignment of carbon nanotubes during the dielectrophoresis process, in AIP Conference Proceedings, AIP Publishing, 1989 (2018) , p. 030008.

[14] J. Kang, S. Hong, Y. Kim, S. Baik, Controlling the carbon nanotube-to-medium conductivity ratio for dielectrophoretic separation, Langmuir, 25 (2009) 12471-12474.

[15] M.-W. Lee, Y.-H. Lin, G.-B. Lee, Manipulation and patterning of carbon nanotubes utilizing optically induced dielectrophoretic forces, Microfluid. Nanofluid. 8(2010) 609-617.

[16] C. Wei, T.-Y. Wei, F.-C. Tai, The characteristics of multi-walled carbon nanotubes by a two-step separation scheme via dielectrophoresis, Diam. Relat. Mater. 19 (2010) 573-577.

[17] A. Abdulhameed, I. Abdul Halin, M.N. Mohtar, M.N. Hamidon, The role of medium on the assembly of carbon nanotube by dielectrophoresis, J. Disper. Sci. Technol. 41 (2020) 1576-1587.

[18] A.K. Naieni, A. Nojeh, Effect of solution conductivity and electrode shape on the deposition of carbon nanotubes from solution using dielectrophoresis, Nanotechnology, 23 (2012) 495606.

[19] A.I. Oliva-Avilés, A. Alonzo-García, V.V. Zozulya, F. Gamboa, J. Cob, F. Avilés, A dielectrophoretic study of the carbon nanotube chaining process and its dependence on the local electric fields, Meccanica, 53 (2018) 2773-2791.

[20] M.H. Nayfeh, M.K. Brussel, Electricity and magnetism, Dover Publications, NY, 2015.

[21] H. Morgan, N. Green, AC electrokinetics: colloids and nanoparticles, Research Studies Press LTD, Hertfordshire, England, 2003.

[22] S.B. Asokan, L. Jawerth, R.L. Carroll, R. Cheney, S. Washburn, R. Superfine, Two-dimensional manipulation and orientation of Acti-Myosin systems with dielectrophoresis, Nano Lett. 3 (2003) 431-437.

[23] H. Morgan, N.G. Green, Dielectrophoretic manipulation of rod-shaped viral particles, J. Electrostat. 42 (1997) 279-293.

[24] C. Wei, T.-Y. Wei, C.-H. Liang, F.-C. Tai, The separation of different conducting multi-walled carbon nanotubes by AC dielectrophoresis, Diam. Relat. Mater. 18 (2009) 332-336.

[25] J.-E. Kim, C.-S. Han, Use of dielectrophoresis in the fabrication of an atomic force microscope

tip with a carbon nanotube: a numerical analysis, Nanotechnology, 16 (2005) 2245-2250.

[26] H. Morgan, A.G. Izquierdo, D. Bakewell, N.G. Green, A. Ramos, The dielectrophoretic and travelling wave forces generated by interdigitated electrode arrays: analytical solution using Fourier series, J. Phys. D Appl. Phys. 34 (2001) 1553-1561.

[27] V.L. Streeter, E.B. Wylie, Fluid Mechanics; SI Metric Ed., McGraw-Hill, NY, 1983.

[28] W.G. Don, H.P. Robert, Perry's Chemical Engineers' Handbook, 8th ed., McGraw-Hill Education, NY, 2008.

[29] H.K. Hansjörg Bipp, Formamides, in Ullmann's Encyclopedia of Industrial Chemistry, Wiley-VCH, 2011.

[30] D.R. Lide, CRC Handbook of Chemistry and Physics, 84th ed., CRC press, NY, 2004.

[31] K. Holmberg, Surfactants, in Ullmann's Encyclopedia of Industrial Chemistry, Wiley-VCH, 2011, pp. 1-56.

[32] R. Schmidt, K. Griesbaum, A. Behr, D. Biedenkapp, H. Voges, D. Garbe, C. Paetz, G. Collin, D. Mayer, H. Höke, Hydrocarbons, in Ullmann's Encyclopedia of Industrial Chemistry, Wiley-VCH, 2014, pp. 1-74.

[33] H. Ertl, R. Ghai, F. Dullien, Liquid diffusion of nonelectrolytes: Part II, AIChE J. 20 (1974) 1-20.

[34] C. Wilke, P. Chang, Correlation of diffusion coefficients in dilute solutions, AIChE J. 1 (1955) 264-270.

[35] G. Chen, Y. Hou, H. Knapp, Diffusion coefficients, kinematic viscosities, and refractive indices for heptane+ ethylbenzene, sulfolane + 1-methylnaphthalene, water + N, N-dimethylformamide, water + methanol, water + N-formylmorpholine, and water + N-methylpyrrolidone, J. Chem. Eng. Data, 40 (1995) 1005-1010.

[36] H. Ertl, F. Dullien, Self-diffusion and viscosity of some liquids as a function of temperature, AIChE J. 19 (1973) 1215-1223.

[37] M. Saghir, C. Jiang, S. Derawi, E.H. Stenby, M. Kawaji, Theoretical and experimental comparison of the Soret coefficient for water-methanol and water-ethanol binary mixtures, Eur. Phys. J. E, 15 (2004) 241-247.

[38] R. Cicoria, Y. Sun, Dielectrophoretically trapping semiconductive carbon nanotube networks, Nanotechnology, 19 (2008) 485303.

[39] C. Zhang, K. Khoshmanesh, A. Mitchell, K. Kalantar-Zadeh, Dielectrophoresis for manipulation of micro/nano particles in microfluidic systems, Anal. Bioanal. Chem. 396 (2010) 401-420.

[40] K. Khoshmanesh, C. Zhang, S. Nahavandi, S. Baratchi, A. Mitchell, K. Kalantar-zadeh, Dielectrophoretically patterned carbon nanotubes to sort microparticles, Electrophoresis, 31 (2010) 3380-3390.

[41] K. Khoshmanesh, C. Zhang, S. Nahavandi, F.J. Tovar-Lopez, S. Baratchi, A. Mitchell, K. Kalantar-zadeh, Size based separation of microparticles using a dielectrophoretic activated system, J. Appl. Phys. 108 (2010) 034904.